

Elucidation of Polyurethane Dispersions in a Batch Rotor-Stator Mixer

Supathorn Phongikaroon** and Richard V. Calabrese—University of Maryland*

Keith Carpenter—Institute of Chemical and Engineering Sciences†

In this study, the effect of high energy input from mechanical agitation, provided with a high shear rotor-stator, on the drop size and the drop size distribution (DSD) of aqueous polyurethane (PU) dispersions is investigated. The effect of the dispersed phase volume fraction (ϕ) on the DSD of aqueous PU dispersions is also examined to understand the fundamental characteristics that result from the high shear mixing. DSD is measured by using either a high magnification video probe or dynamic light scattering, depending on the range of drop sizes. For the PU without any ionic content, the distributions appear to be bimodal with rather large drop sizes. The mean sizes of the first and second modes are about 10 and 22 μm , respectively. For the PU with an ionic content, the mean drop sizes are approximately 80 nm. The distributions reveal that functional chemistry plays a more dominant role in the process of making PU dispersions than the mechanical agitation, and that ϕ has a weak effect on the mean drop sizes. The results further suggest that mechanical agitation can be used to control the breadth of the distributions.

Keywords: Isocyanates, latexes, colloids, emulsions, polyurethanes, waterborne, application characteristics, data analysis, statistics, urethane, dispersion, batch rotor-stator mixers, drop size distribution

The technology of aqueous polyurethane (PU) dispersions has advanced considerably over the past 30 years. Aqueous PU dispersions have become an important process in the surface coating industry because they are nontoxic and nonflammable. In addition, the environmental impact through the air is minimal, relative to solvent-based coatings. Since PU dispersions are used frequently in industrial applications, many of the experiments that define their properties have been carried out in industrial laboratories.¹⁻⁴ Typically, aqueous PU is characterized by a presence of both urethane ($-\text{NH}-\text{CO}-\text{O}-$) and urea ($-\text{NH}-\text{CO}-\text{NH}-$) groups. A reaction of isocyanates (NCO) with water plays a role when dispersing PU⁵:



The formation of carbon dioxide causes severe foaming, which has been shown to affect the polymer properties.^{4,6,7} The amino groups may then react with the remaining isocyanates yielding urea linkages. PU molecules are originally immiscible with water. Thus, certain types of hydrophilic (ionic) groups, such as α,α -dimethylpropionic acid (DMPA), are bound to the polymer as an internal emulsifier. Then a base group, typically triethylamine (TEA), is used to neutralize these acid groups. This technique provides three advantages to PU molecules. First, it requires a low shear force requirement. Second, the result-

ing droplets are fine and small after mixing. Third, the emulsion has good dispersion stability. However, there is a downside to this common procedure. While functional groups serve to solubilize the polymer, they also serve to degrade coating properties because they make the material more hydrophilic, and the fundamental reason for the coating is to make it water resistant.

Previous studies on aqueous PU focused on the general physical chemistry of dispersions and changes of process parameters. Often, stabilized aqueous PU dispersions are produced in stirred tanks by using functional acid groups to solubilize the polymer. However, there are relatively few studies that focus on the effect of high energy input from mechanical agitation on the drop size and drop size distribution of polyurethane dispersions. Thus, the main goal of the experiments is to evaluate this factor by using a high shear rotor-stator mixer. This study will provide useful insight into whether or not the high-energy input from the mechanical agitation of a rotor-stator mixer can produce fine stabilized droplets with fewer additives or functional groups.

EXPERIMENTAL PROCESSES

All the experiments were conducted using a Ross ME 100 LC rotor-stator mixer with a four-bladed rotor, which

* Dept. of Chemical Engineering, College Park, MD 20742.

† 1 Pesek Rd., Jurong Island, Singapore 627833.

** Author to whom correspondence should be addressed. Present address: Remote Sensing Division, Naval Research Laboratory, Washington, D.C. 20375. Email: supathorn@nrl.navy.mil.

NOMENCLATURES

D	drop diameter
D_i	critical diameter
D_M	median diameter
D_{mM}	mass median diameter
D_{max}	maximum drop diameter
D_{nM}	number mean diameter
D_{10}	number mean diameter
D_{30}	mass mean diameter
D_{32}	Sauter mean diameter
D_{43}	mass-weighted mean diameter
$f_n(D_i)$	number frequency to the i^{th} size interval
$f_n(D_i)$	number continuous frequency function = $f(D_i)/dD_i$
L	length
m_j	j^{th} moment
N	rotor speed

GREEK LETTERS

ϕ or ϕ	dispersed phase volume fraction
σ_0	standard deviation for the log-normal distribution
τ	delay time
ω or ω	weighting factor

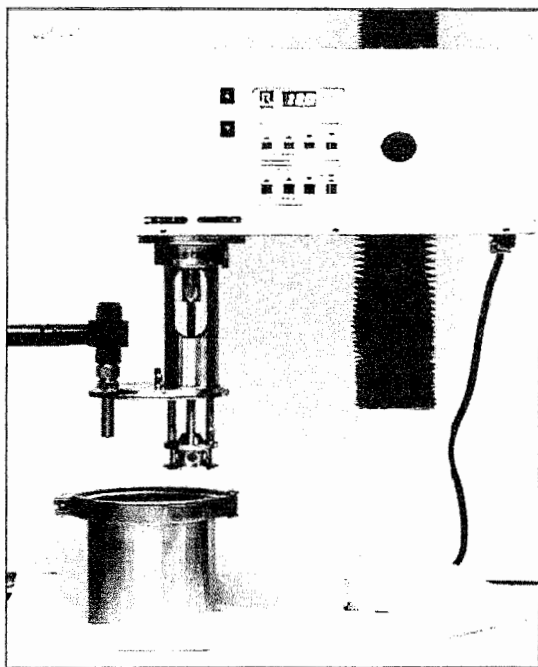


Figure 1—Ross model ME100 rotor-stator mixer with the purpose built stainless steel vessel and the high magnification video probe.

is shown in *Figure 1*. This high shear mixer produces a radial flow pattern. The operating speed range of this mixer is 500–10,000 rpm with increments of 100 rpm. The mixing unit is comprised of a one-HP motor, mixing head, and display panel. It is moved up and down by a separate electrical drive. The preset and actual motor speeds are displayed on the digital readout. The rotor diameter (L) is 3.4 cm with a standard stator inner diameter of 3.5 cm, which gives the standard rotor-stator gap width of 0.5 mm. A slotted stator head is used to produce many fine slot jets in this study. Details of a slotted rotor-stator head are shown in *Figure 2*. The cylindrical tank is a flat-bottom, 2.5-L stainless steel vessel. Francis⁸ provided descriptive details of this rotor-stator mixer.

Temperature control can be achieved by immersing the mixer vessel in a water bath tank. The water is kept at constant temperature using a combination of a heater and cooling water flowing through a recirculation loop. The heater controller (VWR Scientific Model 1112) has fine and coarse scales on the front panel for precise control. The uncertainty of this controller is within $\pm 0.3^\circ\text{C}$.

Two prepolymer products (supplied by Avesia) were used in this study: (1) 0 wt% DMPA (labeled T1) and (2) 7.5 wt% DMPA (labeled T2). Physical properties⁶ of both prepolymer samples are given in *Table 1*. Triethylamine (TEA) was selected to neutralize the $-\text{COOH}$ groups on the 7.5 wt% DMPA prepolymer. Both samples were preheated at 60°C to reduce the viscosity. The water bath temperature was raised and fixed at 60°C . During the preparation, 2.0 L of deionized water was poured into the stainless steel vessel. The vessel was then connected to the motor and placed into the water bath. Sample T1 was prepared in a beaker and poured into the vessel through the funnel into the operating mixer. The dispersed phase volume fractions (ϕ) ranged from 0.01 to 0.10 in this experiment. The dispersion was allowed to react at constant operating conditions while stirring continued at that particular speed. After 90 min, the sample was withdrawn using a syringe and the drop size measurement was accomplished with the high magnification video probe.⁸ The withdrawn sample was diluted with distilled water to accommodate the video probe measurement. The size distribution was characterized using an interlaced Fibonacci series to define bin size from at least 200 counts of the drop diameter.⁹ The rotor speed was then changed from 8000 to 9000 rpm with the same processing time.

For another experiment run, sample T2 was fully neutralized by TEA. The volume ratio of the prepolymer to the TEA became 6.93 to 1. We allowed at least two hours for the system to achieve equilibrium drop size distribution.⁹ The samples were then withdrawn at each rotor speed for the drop size measurement using a dynamic light scattering (DLS) technique. This was done by diluting 50 mL of the withdrawn sample with 3 mL of deionized water. *Table 1* gives a summary of all discussed experimental runs.

RESULTS AND DISCUSSION

Samples of the histograms of number frequency $f_n(D)$ for EXP01, EXP02, and EXP03 at 8000 and 9000 rpm are

Table 1—Experimental Dispersions

Prepolymer Properties	Experimental Runs	ϕ	N (rpm)
T1 (0% DMPA) $\rho = 1003 \text{ kg/m}^3$ $\mu = 3100 \text{ mPa}\cdot\text{s}$	EXP01	0.016	8000 9000
	EXP02	0.052	6000 7000 8000 9000
	EXP03	0.073	8000 9000
T2 (7.5% DMPA) $\rho = 1049 \text{ kg/m}^3$ $\mu = 10,336 \text{ mPa}\cdot\text{s}$	EXP04	0.095	7000 8000 9000
	EXP05	0.101	7000 8000
	EXP06	0.181	8000

plotted in Figures 3 A-F, respectively. These plots reveal that the distributions are bimodal. We speculated that this is a result of coalescence of smaller drops through the transfer process. Previous studies^{3,5,6} have shown that the colloids typical of this dispersion are not stable. To help facilitate the discussion, we used the bimodal distribution approximation technique^{10,11} to analyze these experimental data. This approximation technique is based on the following models:

$$f_1(D) = \frac{1}{\sqrt{2\pi}\sigma_{01}} \exp\left[-\frac{1}{2}\left(\frac{\ln D - \ln D_{M1}}{\sigma_{01}}\right)^2\right] \frac{1}{D} \quad 0 < D < D_{\max} \quad (1)$$

$$f_2(D) = \frac{1}{\sqrt{2\pi}\sigma_{02}} \exp\left[-\frac{1}{2}\left(\frac{\ln D - \ln D_{M2}}{\sigma_{02}}\right)^2\right] \frac{1}{D} \quad 0 \leq D \leq D_{\max} \quad (2)$$

Here, $f(D)$ is a continuous frequency function for the log-normal distribution, σ_0 is the standard deviation for the log-normal distribution, D_M is the median diameter, and D_{\max} is the maximum drop diameter. The subscripts 1 and 2 are denoted for the first and second peaks, respectively. Since both distributions are normalized, the weighting factor method can be employed to obtain unity for the area under the sum of both frequency distribution curves, that is

$$\int_0^{D_{\max}} [\omega(D_1) \cdot f_1(D) + (1 - \omega(D_1)) \cdot f_2(D)] dD = 1 \quad (3)$$

where $\omega(D_1)$ is the weighting factor which is a function of critical diameter (D_1)—where the split of both peaks occurs.

The continuous size distribution functions for all the experimental data sets were first calculated with the initial guess for the weight factor, $\omega = 0.84$. We use the least-square technique to determine the best-fit parameters—the number medians for both peaks and the standard deviations for the log-normal distribution. The resulting geometric standard deviations (GSD) for both peaks were calculated. The mass median diameters (D_{mM}), the number mean diameters (D_{10}), and mass mean diameters (D_{30}), were obtained using the following statistical relationships for a log-normal distribution:

$$m_j = D_m^j \exp\left(\frac{1}{2} \sigma_0^2 j^2\right) = \int_0^\infty D^j f(D) dD, \text{ and} \quad (4)$$

$$D_{mM} = D_{nM} e^{\sigma_0^2 / 2} \quad (5)$$

where m_j is the specified j^{th} moment and D_{nM} is the number mean diameter.

The results are listed in Table 2. These results show that the mean drop sizes (for instance, D_{10} and D_{30}) are independent of N but are dependent on ϕ . After normalizing $f_n(D_1)$, it was possible to compute the average number median and standard deviations for $f_1(D)$ and $f_2(D)$. The rela-

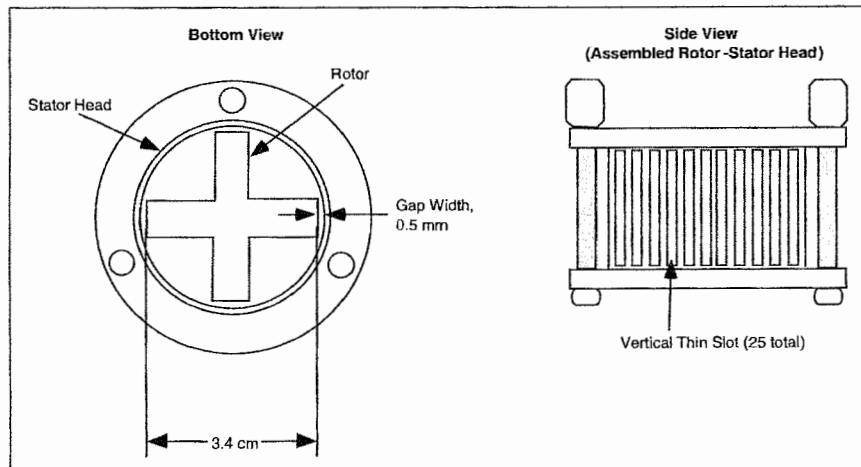


Figure 2—Close-up views of the slotted stator head with dimensions for the Ross mixer.

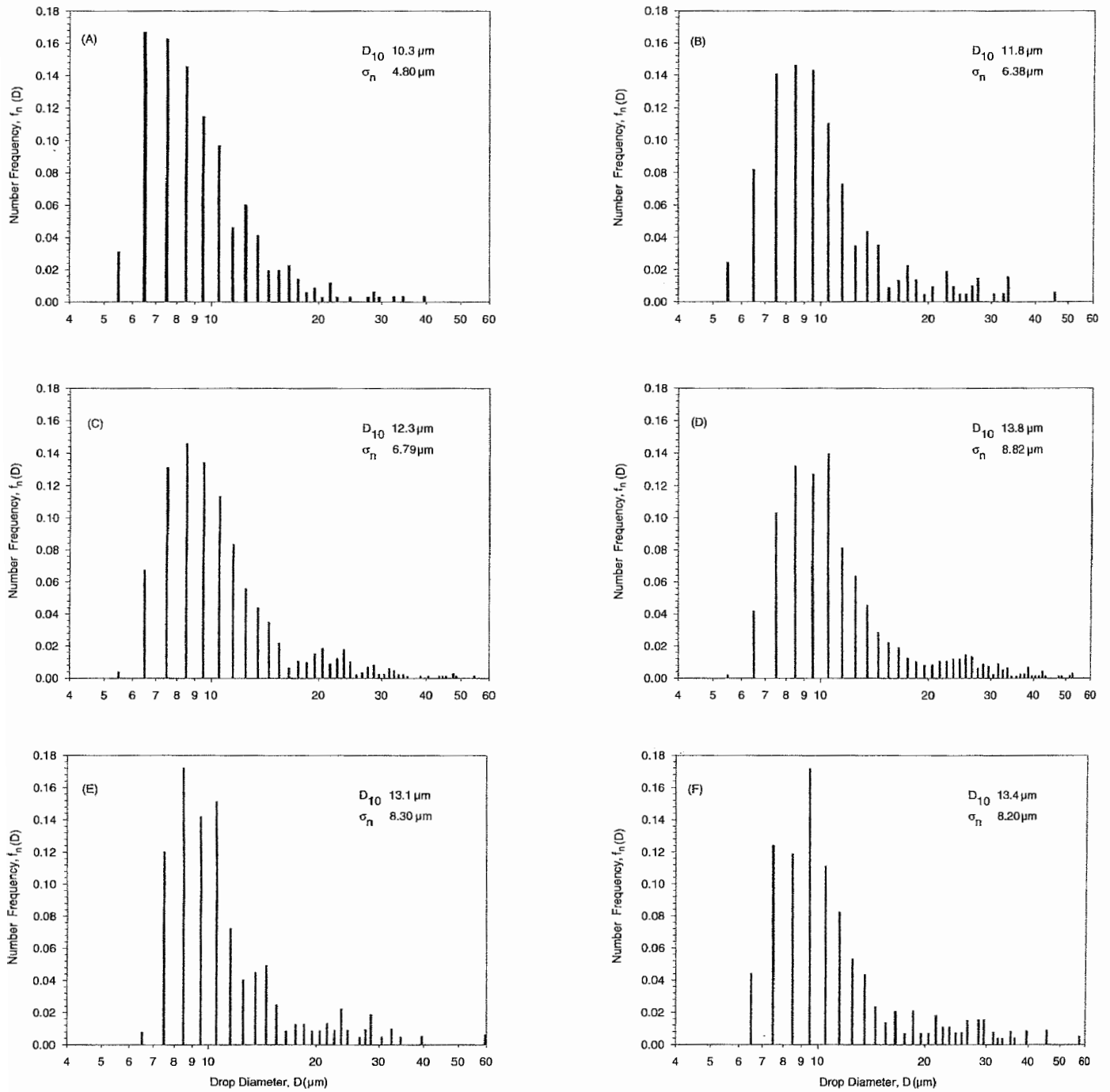


Figure 3—Plots of number frequency for T1 prepolymer dispersions: (A) $\phi = 0.016$, $N = 8000$ rpm; (B) $\phi = 0.016$, $N = 9000$ rpm; (C) $\phi = 0.052$, $N = 8000$ rpm; (D) $\phi = 0.052$, $N = 9000$ rpm; (E) $\phi = 0.073$, $N = 8000$ rpm; and (F) $\phi = 0.073$, $N = 9000$ rpm .

Table 2—Bimodal Approximation Parameters for EXP01 to EXP03

Experimental Run Speed (rpm) Weight Factor	Peak 1					
	D_{nM} (μm)	σ_o (μm)	GSD (μm)	D_{mM} (μm)	D_{10} (μm)	D_{30} (μm)
EXP01, 8000 $\omega = 0.88$	8.50	0.27	1.31	10.59	8.81	9.48
EXP01, 9000 $\omega = 0.84$	9.20	0.26	1.3	11.32	9.52	10.20
EXP02, 6000 $\omega = 0.83$	9.07	0.25	1.28	10.86	9.35	9.92
EXP02, 7000 $\omega = 0.80$	9.54	0.21	1.24	10.30	9.75	10.20
EXP02, 8000 $\omega = 0.83$	9.40	0.25	1.28	11.29	9.69	10.30
EXP02, 9000 $\omega = 0.80$	9.89	0.25	1.28	11.89	10.20	10.84
EXP03, 8000 $\omega = 0.79$	9.62	0.22	1.24	11.06	9.85	10.31
EXP03, 9000 $\omega = 0.80$	9.67	0.24	1.27	11.54	9.96	10.56

Experimental Run Speed (rpm) Weight Factor	Peak 2					
	D_{nM} (μm)	σ_o (μm)	GSD (μm)	D_{mM} (μm)	D_{10} (μm)	D_{30} (μm)
EXP01, 8000 $\omega = 0.88$	20.00	0.26	1.29	24.40	20.67	22.08
EXP01, 9000 $\omega = 0.84$	22.10	0.23	1.25	25.68	22.63	23.79
EXP02, 6000 $\omega = 0.83$	21.06	0.40	1.49	34.03	22.81	26.76
EXP02, 7000 $\omega = 0.80$	21.45	0.26	1.29	26.15	22.17	23.68
EXP02, 8000 $\omega = 0.83$	21.60	0.26	1.30	26.48	22.35	23.91
EXP02, 9000 $\omega = 0.80$	25.14	0.24	1.27	29.75	25.86	27.34
EXP03, 8000 $\omega = 0.79$	20.90	0.24	1.27	24.70	21.49	22.71
EXP03, 9000 $\omega = 0.80$	23.98	0.22	1.25	27.84	24.58	25.8

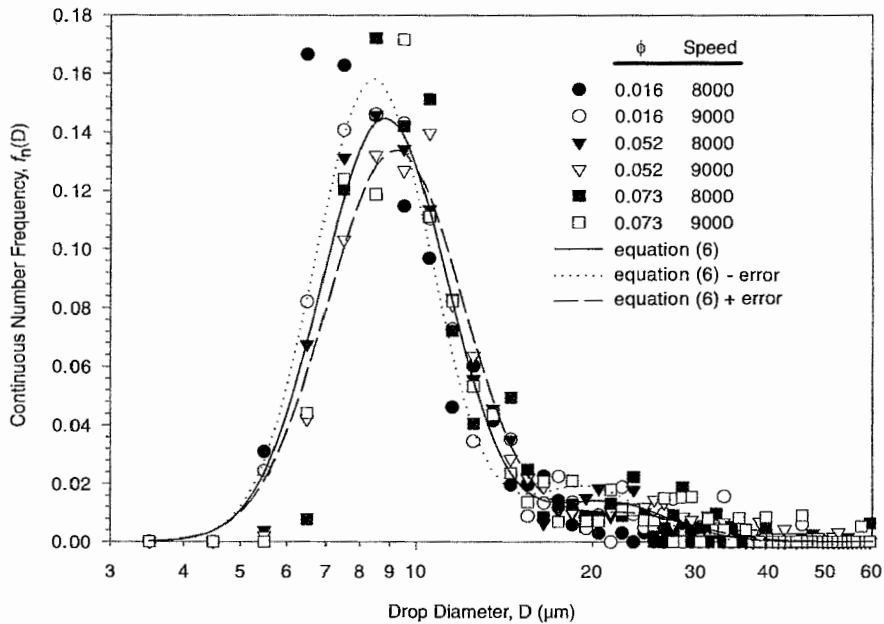


Figure 4—Continuous number frequency plot for T1 prepolymer dispersions. Equation (6) and its \pm calculated standard deviations are superimposed on the data sets. The weight factor ω is 0.82 ± 0.034 .

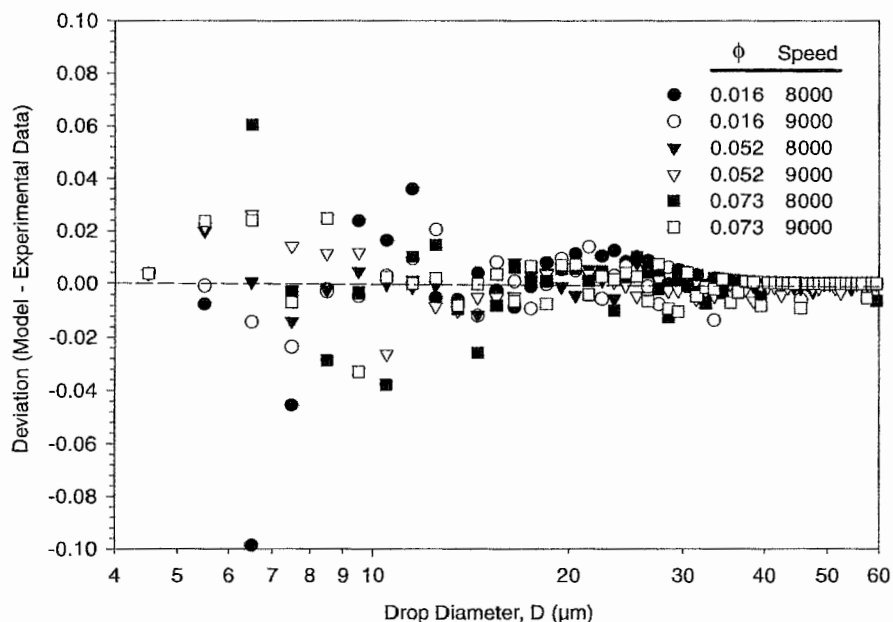


Figure 5—Deviation between equation (6) and experimental data sets.

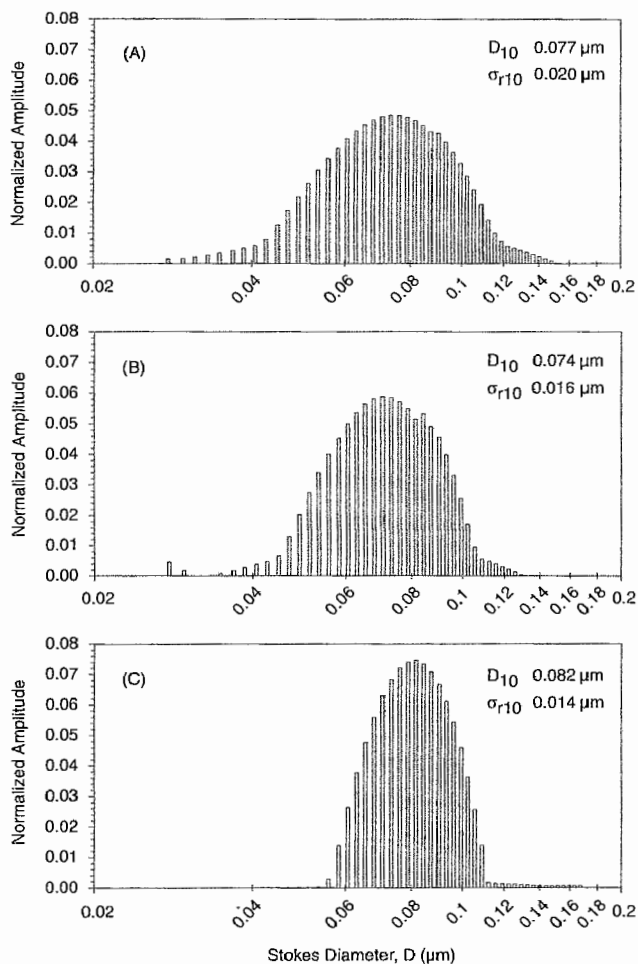


Figure 6—Plots of normalized amplitude with linear mode at ϕ of 0.095 for the fully neutralized T2 prepolymer dispersions, EXP04, at (A) 7000 rpm, (B) 8000 rpm, and (C) 9000 rpm.

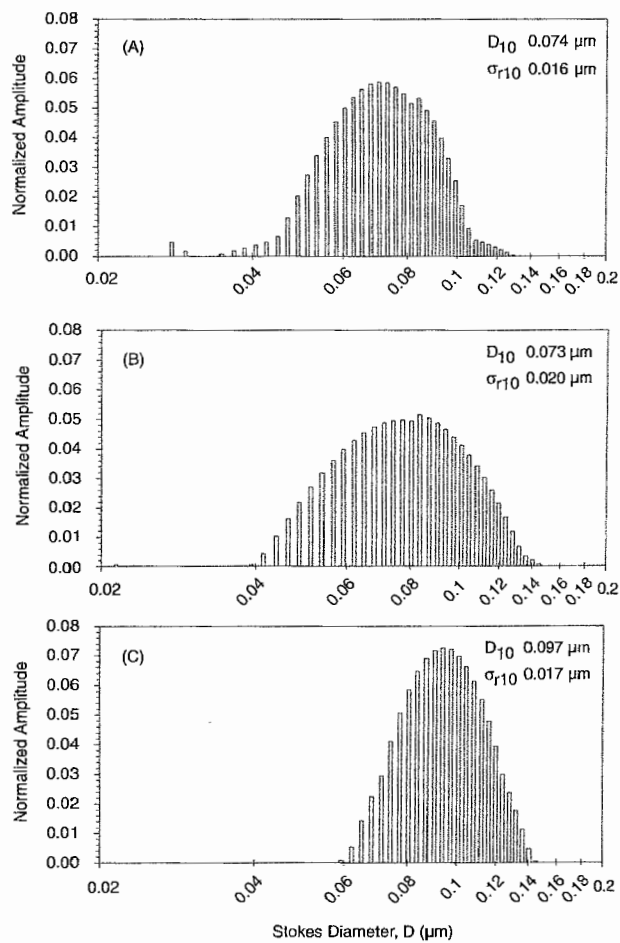


Figure 7—Plots of normalized amplitude with linear mode for the fully neutralized T2 prepolymer dispersions at 8000 rpm: (A) EXP04, $\phi = 0.095$; (B) EXP05, $\phi = 0.10$; and (C) EXP06, $\phi = 0.18$.

relationship $f_n(D)$ for these experimental data sets can be expressed as follows:

$$f_n(D) = \frac{\omega}{\sqrt{2\pi(0.25 \pm 0.019)}} \exp\left[-\frac{1}{2}\left(\frac{\ln(D) - \ln(9.38 \pm 0.49)}{0.25 \pm 0.019}\right)^2\right] \frac{1}{D} + \frac{1-\omega}{\sqrt{2\pi(0.24 \pm 0.015)}} \exp\left[-\frac{1}{2}\left(\frac{\ln(D) - \ln(22.28 \pm 1.93)}{0.24 \pm 0.015}\right)^2\right] \frac{1}{D} \quad (6)$$

The average value of ω is 0.82 ± 0.034 . The area under equation (6) is normalized. Without any additives, the result indicates that 80% of the drop population has an average mean diameter of about 10 μm and 20% of that has an average mean diameter of about 22 μm . Figure 4 shows equation (6) plotted with experimental data for 8000 and 9000 rpm at different ϕ to illustrate the degree of scatter. Figure 5 shows the deviation of several experimental data sets and equation (6).

For EXP04 to EXP06, the observed dispersed phase samples consisted of small drops that were stable over several hours. The DLS technique with the linear mode was employed to classify the distribution.¹² Detailed discussion of this experimental method can be found in reference 9. The sample time, τ , was 20 μsec . Four autocorrelation functions were measured at each speed, each data run lasting 10 min for a total of 40 min of data collection. The histogram plots of the distributions of EXP04 are shown in Figures 6 A-C. The results show that the average mean drop diameter is approximately 80 nm. The mean drop sizes of the prepolymer with an ionic content are shown to be approximately 150 times smaller than that of the prepolymer without the ionic content. Similar observation was reported by Satguru and co-workers.³ This observation suggests that, in this system, D_{10} is not a function of energy dissipation from mechanical agitation and that functional chemistry plays a more dominant role than agitation. However, as N increases the distribution becomes narrow around the same mean; that is, the coefficient of variation ($cv = \sigma/D_{10} \times 100$) decreases from 26% at 7000 rpm to 17% at 9000 rpm. As shown in Figures 6 A and B, the distributions have tails of both larger and smaller drops. This implies that high shear mixing can be useful in controlling the breadth of DSD. Comparison of EXP04, EXP05, and EXP06 at 8000 rpm is shown in Figure 7. The results show that D_{10} increases as ϕ increases. By doubling ϕ , D_{10} increases by approximately 30% (see Figures 7A and 7C). The cv for each distribution is approximately 20%.

SUMMARY

An experimental study was performed using a high shear rotor-stator mixer to investigate the effect of mechanical agitation, coupled with the role of functional chemistry, on the DSD of aqueous PU during the dispersion process. As expected, the addition of functional groups to the dispersion reduced the mean drop size in the dispersion. The dispersion process resulted in a bi-

modal distribution in the drop size of the PU for the non-ionic system. The distance between the mean sizes of each mode was approximately 10 μm . For the system with functional chemistry, the mean drop size was about 80 nm. Although the mechanical agitation plays no significant role in the mean drop size, which is a function of dispersed phase volume fraction and functional chemistry, it is responsible for the breadth of the drop size data. Increases in N were shown to drastically alter the cv of the data by producing a tighter range of drop sizes as the mechanical agitation was increased. Thus, high shear mixing can be used to provide an additional control of the DSD without subjecting the system to added functional chemistry, which may impair final coating properties.

ACKNOWLEDGMENTS

Financial support from AstraZeneca and Avecia via Strategic Research Fund No. 269, the University of Maryland High Shear Mixing Research Program: Industrial Advisory Board, and the National Research Council are gratefully acknowledged. The authors would like to thank Dr. K. Peter Judd and Mr. Gregory M. Fike for contributing important suggestions.

References

- Dieterich, D., "Aqueous Emulsions, Dispersions and Solutions of Polyurethane Synthesis and Properties," *Prog. Org. Coat.*, 9, 281 (1981).
- Rosthauser, J.W. and Nachtkamp, K., "Waterborne Polyurethanes," *J. Coated Fabrics*, 16, 39-79 (1986).
- Satguru, R., McMahon, J., Padgett, J.C., and Coogan, R.G., "Aqueous Polyurethanes—Polymer Colloids with Unusual Colloidal, Morphological, and Application Characteristics," *JOURNAL OF COATINGS TECHNOLOGY*, 66, No. 830, 47-55 (1994).
- Kim, B.K., "Aqueous Polyurethane Dispersions," *Colloidal Polym. Sci.*, 274, 599-611 (1996).
- Dieterich, D., "Polyurethane Coatings from Aqueous Dispersions," *Proc. Third International Conference in Organic Coating Science and Technology* (Vol. 1—Advances in Organic Coatings Science and Technology Series), Parfitt, G.D. and Patsis, A.V. (Eds.), Technomic Publishing Co., Greece, 55-76 (1979).
- Saw, L.K., "Phase Inversion of Polyurethane Prepolymer-Water Dispersions," Ph.D. Dissertation, Loughborough University, Loughborough, England, 2000.
- Saw, L.K., Brooks, B.W., Carpenter, K.J., and Knight, D.V., "Different Dispersion Region During the Phase Inversion of an Ionomeric Polymer-Water System," *J. Colloid Interface Sci.*, 257, 163-172 (2003).
- Francis, M.K., "The Development of a Novel Probe for the in situ Measurement of Particle Size Distributions, and Application to the Measurement of Drop Size in Rotor-Stator Mixers," Ph.D. Dissertation, University of Maryland, College Park, MD, 1999.
- Phongikaroon, S., "Drop Size Distribution for Liquid-Liquid Dispersions Produced by Rotor-Stator Mixers," Ph.D. Dissertation, University of Maryland, College Park, MD, 2001.
- Irani, R.R. and Callis, C.F., *Particle Size: Measurement, Interpretation, and Application*, Wiley and Sons, New York, 1963.
- Dallavalle, J.M., Orr, C.J., and Blocker, H.G., "Fitting Bimodal Particle Size Distribution Curves," *Industrial and Engineering Chemistry*, 43, 1377 (1951).
- Danheke, B.E., *Measurement of Suspended Particles by Quasi-Elastic Light Scattering*, Wiley-Interscience: New York, 1983.